International Journal of Security and Its Applications
Vol. 9, No. 3 (2015), pp. 153-162
http://dx.doi.org/10.14257/ijsia.2015.9.3.15

# An Iris Localization Algorithm based on Morphological Processing

Kun Yu[1], Zeyu Xu[2] and Lixin Xu[1]

*1 Henan Mechanical and Electrical Engineering College, Xinxiang 453002,China*
*2 College of Material Science and Engineering, Zhengzhou University, Zhengzhou 450001, China*
*2315306@qq.com*

***Abstract***

*To improve the speed of iris localization, an iris localization algorithm based on the morphological processing is proposed with fast speed. Firstly, pupil area is segmented from eye image by thresholding, to remove eyelash noise and other noises from binaryzation pupil area by morphological open operation. Then, a series of structure element of radius increasing is used to make morphological erode operation on pupil area to localize roughly the inner boundary of the iris. Finally, calculus operator is employed to accurately localize the inner and outer iris boundary. 108 iris images from CASIA (Version 1.0) iris database are used to do iris localization experiments. The localization accurate rate of the proposed algorithm, calculus operator and hough transform is 97.2%, 90.3% and 92.1% respectively. Experiment results have showed that the proposed algorithm has a high performance on speed and precision with strong robustness to the different quality iris images.*

***Keywords:*** *iris localization, calculus operator, morphological method, hough transform*

## 1. Introduction

Iris recognition is regarded as the most secure and the most accurate method. It uses the texture features of iris eyes in the image (ring, wrinkles, spots, and coronal) to form the feature template and complete identification through comparing the iris sample feature with feature template [1].

Iris is an annular region between the pupil and sclera, There exists an obvious grayscale change between the pupil, iris and sclera boundary, which provides the possibility for the iris edge detection. Iris localization is the process of determining inner and outer boundaries of the iris, which will directly influence the accuracy and speed of iris recognition. Iris boundary localization is shown in Figure 1

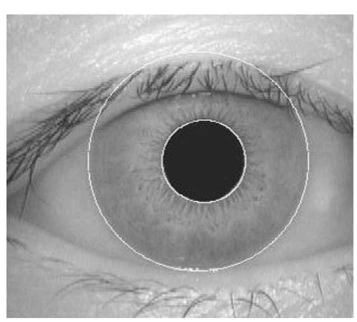

**Figure 1. Iris localization**

ISSN: 1738-9976 IJSIA

At present, traditional iris localization methods use the detection of circle edge operators to extract inner and outer edges of iris including calculus operator algorithm proposed by Daugman [2], hough transform algorithm based on binaryzation proposed by Wildes [3], the least square algorithm proposed by Wang [4], and localization algorithm based on geometric features [5]. The former two kinds of algorithms are classic iris localization algorithms. The calculus operator algorithm uses gradient information, when image illumination has changes, there is no question of choosing threshold value, but it is easy to be influenced by the image point of light source and light spots so that localization fails. The hough transform depends on the selection of binarization boundary points. The clarity and contrast degrees of the image are easily affected by illumination to produce false boundary, which causes uncorrected localization of the iris boundaries

The above two kinds of classic algorithms have problems of slow localization speed and uneven illumination influence. The least square algorithm belongs to the parameter fitting with fast localization speed, but the localization accuracy is lower than the two formers. Besides the above algorithms, there are some improved algorithms. The main principle is to reduce the search space of the calculus operator algorithm to improve the localization speed, or accurately extract the more edge points fitting in order to improve the localization accuracy [6]. Some scholars also think that the pupil with the growth of age become the oval [7]. The oval is employed to define the characteristics of the pupil [8], to achieve higher localization accuracy. However, compared to determine the three parameters of the circle, the oval is determined, which requires five parameters, so that the computational complexity increases. Therefore, the localization speed should be discussed further.

Because of the slow speed of the calculus operator and hough transform in iris localization, an iris localization algorithm with fast speed and high accuracy is proposed based on the morphological processing, combing with the coupling of the inner and outer edge and narrow the search range of the outer edge by the calculus operator algorithm, so as to reduce the amount of calculation. the localization effect of proposed algorithm is more superior than that of the classical calculus algorithm and hough transform algorithm.

## 2. Iris Inner Boundary Localization

### 2.1 Iris Image Smoothing Processing

In order to achieve the double aims of protecting the iris boundary information and removing the noise, the weighted filter is generally used for smoothing filter to the image. In the weighted filter commonly used, gauss filter is very typical with the good filtering effect, which can filter the noise and protect the boundary information of the goal. Coefficients of gauss filter and the distance from the filter center is inversely proportional. The discrete gauss template can be obtained by the two-dimensional continuous gauss function in Formula (1) after sample, quantization and template normalization.

$$G(x, y) = \frac{1}{2\pi\sigma^2} e^{-\frac{x^2 + y^2}{2\sigma^2}} \quad (1)$$

In the filtering process, the filter center glides over the iris image. The grayscale of an iris image points corresponding to the center of the filter is equal to the sum of the gray filter coefficient multiplying the gray value corresponding pixel. Standard deviation $\sigma$ determines the “steep degree” of the gauss function. The bigger $\sigma$ is; the more obvious low passing filtering effect and after smoothing, the more blurred the iris image details are, two-dimensional gauss distribution is shown in Figure 2. The process effect is better than the mean filter. We can obtain the more gentle smoothing effect not to damage the boundary in the image, which can eliminate the high frequency noise of the original iris image.

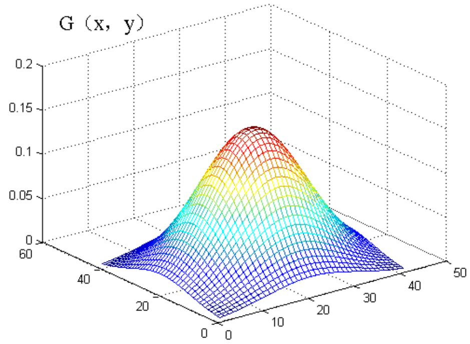


**Figure 2. Two-dimensional Gauss Distribution**

### 2.2 The Rough Localization of Iris Inner Boundary

The threshold segmentation method is employed primarily to extract the pupil region, and then morphology open operation is done for the iris image to eliminate the noise interference of the eyelash and spots.

Figure 3 is a typical histogram of human eye image, and the histogram shows that the eye image grayscale distribution has some characteristics. The pupil grayscale value is less than the iris grayscale value, iris grayscale value is less than the sclera grayscale value, and the pupil grayscale value is concentrated in a narrow range, which shows a sharp peak in the histogram. According to formula (2), the human eye image is for the threshold, in which $I(x, y)$ is the grayscale value of the point $(x, y)$; $T$ is the segmentation threshold; threshold $T$ is selected on the right of the first peak in the histogram; $BW$ is an image after thresholding. Figure 4 is the result after thresholding. According to the results, the pupil is separated more completely, and a little edge of eyelids and of eyelashes is also separated.

$$\begin{cases} BW(x, y) = 0 & \text{if} \quad I(x, y) < T \\ BW(x, y) = 1 & \text{if} \quad I(x, y) > T \end{cases} \tag{2}$$

In Figure 4, the outside of the pupil has a part of noise in the eyelash area, and the pupil boundary is not so smooth, and the morphological opening operation is the first corrosion to the image and then expansion to the image. The corrosion can eliminate the narrow protrusion and the fine protrusion which is smaller than structural elements [9], such as the thin eyelashes in Figure 4. The same structure elements are expanded to recover the corroded area of the original pupil, which makes the edge smoother.

 

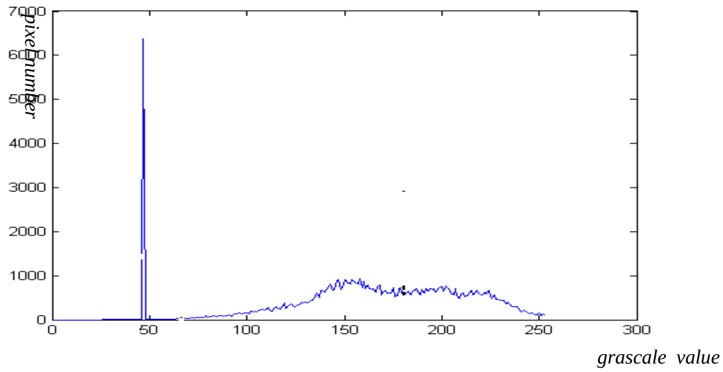


**Figure 3. The Eye Image Histogram**

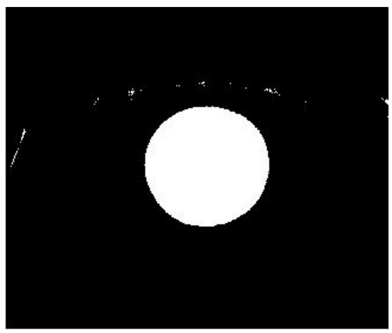

**Figure 4. The Result of Threshold Segmentation**

Morphological opening operation: $BW \circ B = (BW \Theta B) \oplus B$ (3)

Corrosion operation: $BW \Theta B = \{z \mid (B)_z \subseteq BW\}$ (4)

The expansion operation: $BW \oplus B = \{z \mid (\hat{B})_z \cap A \neq \varnothing\}$ (5)

BW is the image of thresholding image, and *B* is a structure element of the disc type radius for 5. $(B)_z$ represents point *z* to *B* translation, and $\hat{B}$ represents the image of *B*. opening operation results of Figure 4 are shown in Figure 5. It can be seen that the eyelash noise of the outside pupil area after opening operations is eliminated, and the boundary of the pupil region becomes smoother.

The row and column scanning is carried out for the pupil area after morphological opening operation as shown in Figure 6. The two longest chords $L_1$ and $L_2$, are found in the horizontal direction and the vertical direction, whose length is $L_{10}$ and $L_{20}$ respectively. In fact, the lengths of two chords is the approximate diameter of the pupil, but due to the non-smoothness of pupil area boundary, to ensure the accuracy, n chords are withdrawn nearby $L_1$ and $L_2$, whose length is: $\{L_{10}, L_{11}, \ldots, L_{1n}\}, \{L_{20}, L_{21}, \ldots, L_{2n}\}$. The mean value of $2(n+1)$ chords length is the $L_p$ of initial diameter of the pupil, and then the radius of the initial of the pupil:

$$r_p = \frac{L_p}{2} \tag{6}$$

$$L_p = \frac{\sum_{i=0}^{n} L_{1i} + \sum_{i=0}^{n} L_{2i}}{2(n+1)} \tag{7}$$

 

The systematical structural element is used to do morphology corrosion to the pupil area. The $2m$ disk structure element $\{ B_1, B_2, \cdots, B_m, \cdots, B_{2m} \}$ is applied to do morphology corrosion to the pupil area as shown in Figure 5, and the radius $r_j$ of $j$ structural elements $B_j$ meets:

$$\begin{cases} r_j = r_p - m - j & j \le m \\ r_j = r_p + j - m & j > m \end{cases} \tag{8}$$

With the gradual increase of radius $r_j$ of disc structural elements $B_j$, the morphological erosion operation makes the pupil area smaller and smaller, until it disappears as shown in Figure 7. When structural elements $B_j$ will completely corrode the pupil area. After the structural elements $B_{j-1}$ corrode pupil region, there exists the region of white pixels $A_{j-1}$. rough radius of the pupil $R_p$ is regarded as the structure of the elements $B_j$ corresponding to the radius $r_j$. The pupil center $(x_p, y_p)$is defined as the centroid of $A_{j-1}$ area. $p(x_j, y_j)$ is a point in $A_{j-1}$ and $S_{j-1}$ is the area of $A_{j-1}$, which is the number of pixels of region $A_{j-1}$.

$$\begin{cases} A_i = \sum_{p \in L_i} 1 \\ x_p = \dfrac{\sum_{p \in L_i} x_j}{A_i} \\ y_p = \dfrac{\sum_{p \in L_i} y_j}{A_i} \end{cases} \tag{9}$$

The obtained parameters are used to rough localization results of pupil such as shown in Figure 8.

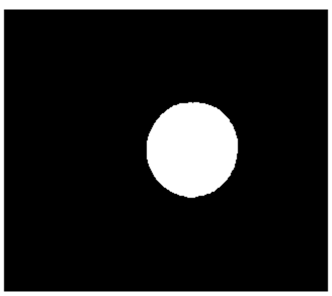

**Figure 5. Open Operation Results**

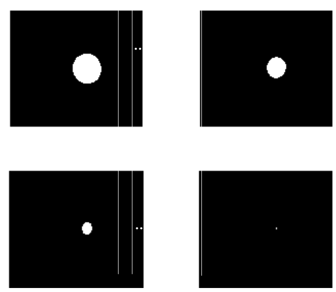

**Figure 6. Scanning Process of Row and Column**

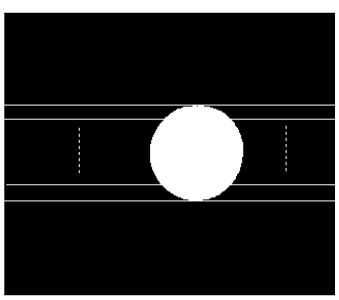

**Figure 7. The Corrosion Process**

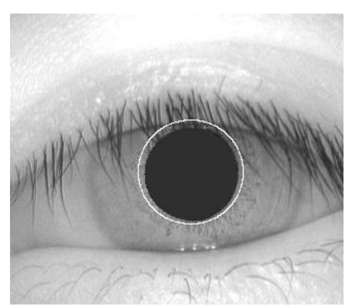

**Figure 8. The Rough Location of the Inner Edge**

## 3. The Precise Localization of Iris Inner Boundary

Based on the rough location of the iris inner edge, Daugman circular gradient algorithm is adopted to get further the precise location. As the pupil edge is darker than its surrounding, so in the literature [3], the circle gradient operator can precisely localizing the inner edge.

$$\max_{(r,x_0,y_0)} |G_\sigma(r) * \frac{\partial}{\partial r} \oint_{(r,x_0,y_0)} \frac{I(x,y)}{2\pi r} ds \qquad (10)$$

$I(x,y)$ represents the graysacle value of the iris image in pixels $(x,y)$. The operator regards $(x_0,y_0)$ as the center to search possible radius $r$, and calculates difference value of the grayscale average value between two adjoining circumferences. When difference value gets the maximum, the corresponding parameters $(x_0,y_0,r)$ is the iris boundary. Which is searched for. In formula (11), * is the convolution operation, and $G_\sigma(r)$ is the smooth operator of the standard deviation $\sigma$ , to play a smooth filtering role.

$$G_\sigma(r) = (1/\sqrt{2\pi}\sigma)e^{\frac{-(r-r_0)^2}{2\sigma^2}} \qquad (11)$$

$x_0 \in (x_p\text{-}15, x_p\text{+}15), y_0 \in (y_p\text{-}15, y_p\text{+}15), r \in [r_p\text{-}15, r_p\text{+}15]$, $(x_p, y_p, r_p)$ are rough localization results of the pupil parameters and finally the accurate parameters for the iris inner boundary is $(X_P,Y_P,R_P)$.

## 4. The Localization of Iris Outer Boundary

The transition band of iris outer boundary is often wide and its rich texture information of the iris will also affect the iris outer boundary localization [10], so that direct application of formula (10) sometimes cannot accurately localize the iris outer boundary. The proposed algorithm adopts the surface integral formula of the form as formula (12) instead of formula (10) line integral to gain the precise localization of the iris outer boundary.

$$\max_{(r,x_0,y_0)} |G_\sigma(R) * \frac{\partial}{\partial R} \iint_D \frac{I(x,y)}{\pi R^2} d\delta | \qquad (12)$$

Because the inner and outer boundary of iris cannot be considered a concentric circle, the center distance is less than $d$ [10].Here $d$=20, the surface integral algorithm is used to localize the iris outer boundary, and the search range of the parameters are $x_0 \in [x_p\text{-}10, x_p\text{+}10]$, $y_0 \in [y_p\text{-}10, y_p\text{+}10]$. Because radius $r$ of the iris outer boundary changes within a certain range, the experience value of $r \in [100, 140]$. In the normal state of human eye gazing, the upper and lower eyelids will cover a portion of the iris, so that the integral region is generally limited in $[-\pi/4, \pi/4]$ and $[3\pi/4, 5\pi/4]$. Finally, the outer boundary parameters get $(X_o, Y_o, R_o)$.

## 5. The Results and Analysis of Experiments

Before localizing the iris, 5×5 size of the template is chosen, Gauss low pass filter of standard deviation σ=1 is used for smooth denoising of the iris image. The experimental image samples from CISIA (Version 1.0) iris database [11], include 108 different eye images. Eye images are completed by the non-contact iris collection device. Collecting distance is about 4~5 cm, and the size of image 280 * 320 pixel.The localization accuracy rate and speed of the proposed algorithm, calculus operator and hough transform is shown in Table 1. The localization results by the proposed algorithm on the different quility of iris images are shown in Figure 9. The effect of the localization to Figure 9 by the three kinds of algorithms is shown in Table 2.

 

**Table 1. The Performance of Iris Localization by the Proposed algorithm**

| Algorithm | Accuracy rate /% | Average localization time /s |
|---|---|---|
| calculus operator | 90.3 | 5.9 |
| hough transform | 92.1 | 4.7 |
| The algorithm proposed | 97.2 | 2.3 |

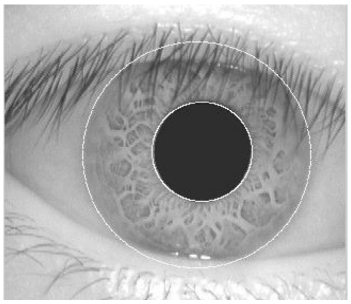

(a) the clear eye image

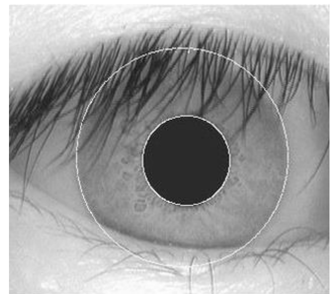

(b) the eye image interfered by the eyelash

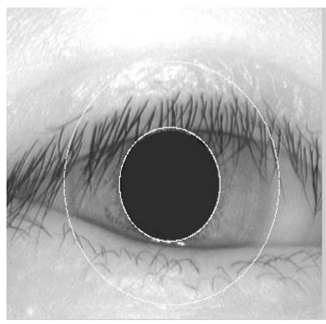

(c) the eye image covered by the eyelids

**Figure 9. Localization Results of the Different Quality Iris Images by the Proposed Algorithm**

**Table 2. The Performance of the Localization to Figure 9 by the Three Kinds of Algorithms**

| eye image | algorithm | iris inner boundary parameters | | | iris outer boundary parameters | | | used time |
|---|---|---|---|---|---|---|---|---|
| | | $X_p$ | $Y_p$ | $R_p$ | $X_o$ | $Y_o$ | $R_o$ | |
| Figure 9(a) | hough transform | 135 | 183 | 39 | 133 | 181 | 103 | 5.2s |
| | calculus operator | 135 | 183 | 38 | 132 | 182 | 103 | 4.1s |
| | the proposed | 136 | 183 | 38 | 136 | 178 | 101 | **1. 7s** |
| Figure 9(b) | hough transform | 150 | 178 | 44 | 154 | 174 | 104 | 5.6s |
| | calculus operator | 150 | 177 | 44 | 145 | 174 | 105 | 4.3s |
| | the proposed | 150 | 177 | 43 | 147 | 173 | 105 | **2.4s** |
| Figure 9(c) | hough transform | 140 | 192 | 56 | 145 | 197 | 105 | 6.4s |
| | Daugman | 140 | 192 | 57 | 140 | 189 | 112 | 5.1s |
| | the proposed | 140 | 193 | 56 | 136 | 193 | 107 | **2.1s** |

 

## 6. Conclusion

The experimental results show that the proposed algorithm uses the threshold to segment human eye image and extract the pupil. After morphological opening operation to remove the noise points, a series of morphological operations are used to roughly localize the pupil edge. Finally, the center coupling the iris inner and outer boundaries as the prior knowledge is used to narrow circular operator search range of the iris outer boundary center. Through the proposed algorithm, the search range of circular gradient operator is greatly reduced, which saves the location time. Based on localizing 108 iris images of CASIA (version 1.0), the results have shown that the proposed algorithm is superior to the classical algorithm of hough transform and calculus operator in iris localization. How to find a practical algorithm is the content and direction of the future study.

## References

[1] Q. Tian, "Review of biological feature recognition", Application research of computers, vol. 26, no. 12, (**2009**), pp. 4404.
[2] J. Daugman, "How iris recognition works", IEEE Transactions on Circuits and Systems for Video Technology, vol. 14, (**2004**), pp. 21-30.
[3] R. Wildes, "Iris recognition: an emerging biometric technology", Proc. IEEE, vol. 85, **(1997**) September, pp. 1348–1363.
[4] L. Ma, Y. Wang and T. Tan, "Biometrics personal identification based on iris pattern", Acta Automatica Sinica, vol. 28, no. 1, (**2002**), pp. 1-10.
[5] C. R. Wang, Z. P. Hu and Q. S. Lian, "An iris location algorithm", Journal of Computer Aided Design & Computer Graphics, vol. 14, no. 10, (**2002**), pp. 950-952.
[6] Z. Ma and H. Wei, "Curve, fitting algorithm for iris localization research", Journal of University of Electronic Science and technology, vol. 38, no. 3, (**2009**),pp. 427-429.
[7] J. F. He and L. S.Zheng, "Iris location", Journal of image and graphics, vol. 5, no. 3, (**2011**), pp. 253-255.
[8] J. H. Wu, D. X .Zhou and J. H. Li, "A fast and precise iris location method", Chinese Journal of scientific instrument, vol. 28, no. 8, ( **2012**), pp. 1469-1473.
[9] "Iris recognition method based on morphological transformation theory", Chinese Journal of scientific instrument, vol. 27, no. 6, (**2006**), pp. 2308-2309.
[10] X. M. Zheng and Y. B. Hou, "A new method of iris location", Journal of Sensing technology, vol. 20, no. 1, (**2007**), pp. 82-84.
[11] "Institute of Automation, Chinese Academy of Sciences", CASIA iris image database (ver1.0) [DB], **(2014)**, http://www.sinobiometrics.com.

## Authors

**Kun Yu**, received his Master Degree from Wuhan University of Technology in 2010.He is now a lecturer of Henan Mechanical and Electrical Engineering College in China. His research interests include software engineering, Network technology and information processing. He has published more than 6 papers on journals and conferences.

**Zeyu Xu**, He is now an Undergraduate student of Zhengzhou University, His professional direction is Material Science and Engineering.

**Lixin Xu**, received his Master Degree from Xi`an Jiaotong University in 2003. He is now a professor of Henan Mechanical and Electrical Engineering College in China. His research interests include electronic government affairs, Network security and information processing. He has published more than 30 papers on journals and conferences.